Expanding the genetic toolbox to explore redox signalling

FINAL REPORT MAJOR RESEARCH PROJECT

Sep. 2020 – Oct. 2021

TESSA VREEMAN
(5878551)

Master student Cancer, Stem Cells & Developmental Biology, Utrecht University

Daily supervisor: D.M.K. van Soest
Examiner: dr. T.B. Dansen
Dansen group, Center for Molecular Medicine, UMC Utrecht
Second reviewer: dr. M.J. Rodríguez-Colman

Table of contents

List of abbreviations

5-FU	5-Fluorouracil
DAAO	D-amino acid oxidase
ETC	Electron transport chain
GFP	Green fluorescent protein
HAP-1	Haploid cell line derived from KBM-7 Chronic Myeloid Leukaemia cells
H_2O_2	H2O2
IMS	Intermembrane space (mitochondrial)
IRES	Internal ribosomal entry site
MDCK	Madin-Darby Canine Kidney cells
MLS	Mitochondrial localisation signal (mitochondrial matrix)
NES	Nuclear exclusion signal (cytoplasmic)
NLS	Nuclear localisation signal (nuclear)
PI	Propidium iodide
ROS	Reactive oxygen species
RPE	Retinal pigment epithelium
MSI organoids	Mouse small intestinal organoids
SOD	Superoxide dismutase
Trx	Thioredoxin
YFP	Yellow fluorescent protein

Layman's summary

In het menselijk lichaam vinden talloze verschillende processen plaats. Deze processen kunnen niet ongecoördineerd plaatsvinden en cellen en weefsels zijn daarom afhankelijk van communicatie onderling. Deze communicatie vindt plaats via signaalmoleculen en eiwitten, die onderdeel zijn van zogenaamde signaalroutes. Een signaalmolecuul kan eiwitten modificeren en deze modificatie zorgt ervoor dat het eiwit actief of inactief raakt en zo signaalroutes kan beïnvloeden. Ook de locatie van een signaalmolecuul in de cel kan bepalen of signalen wel of niet kunnen worden doorgegeven.

Reactieve zuurstofcomponenten (ROS) zijn een groep van reactieve moleculen die betrokken zijn bij het uitwisselen van elektronen rondom zuurstof. Chemische reacties waarbij elektronen worden uitgewisseld worden redox-reacties genoemd. Er werd vaak gedacht dat deze ROS enkel schadelijk is voor de cel: het zorgt voor DNA schade en ontregelingen in signaalroutes, wat kan leiden tot bepaalde ziektes, zoals kanker. Tegenwoordig is het duidelijk dat ROS in hoge concentraties kan zorgen voor schade, maar in lage, fysiologische concentraties het juist als signaalmolecuul functioneert. Daarbij draagt het bij aan belangrijke processen, als cel vermenigvuldiging of cel specialisatie. De belangrijkste ROS is waterstof peroxide (H_2O_2). Er wordt veel onderzoek gedaan naar H_2O_2 als signaalmolecuul in redox-reacties en welke rol H_2O_2 speelt in verschillende processen. Om dit onderzoek uit te voeren worden verschillende hulpmiddelen, of tools, ontwikkeld om de situatie zoals deze zich in het lichaam afspeelt, te modelleren. In het onderzoek dat in dit verslag wordt gepresenteerd wordt een aantal nieuwe tools gemaakt en getest in celmodellen, zodat in de toekomst experimenten gedaan kunnen worden om de rol van ROS beter te begrijpen.

De tools die worden gebruikt, zijn genetisch gecodeerd in een stuk DNA. Dit DNA is vervolgens ingebracht in de cellen, waardoor de tool permanent aanwezig is in de cel. Daarnaast kunnen we deze DNA code aanpassen, zodat de tool op specifieke plekken in de cel aanwezig is. Een van de twee tools is een fluorescente waterstof peroxide sensor, HyPer7. Met deze sensor kunnen we met behulp van fluorescentiemicroscopie H_2O_2 en redox-reacties volgen in de cel. Veel onderzoek wordt gedaan op cellijnen die tweedimensionaal groeien op een petrischaal, maar sommige processen, zoals hoe een weefsel zich vormgeeft, vinden alleen plaats in driedimensionale (3D) celmodellen. Daarom hebben we deze sensor nu ook in 3D-celmodellen gestopt en is er getest of de sensor goed werkt op verschillende plekken in de cel. Daarnaast is de sensor gebruikt om ROS productie na het behandelen van cellen met een chemotherapie te visualiseren. Verschillende chemotherapieën maken gebruik van het feit dat ROS in hoge concentraties zorgt voor schade, met name in snelgroeiende cellen, zoals kankercellen. De andere tool die is gebruikt, is een enzym genaamd D-aminozuur oxidase (DAAO). Dit enzym kan in aanwezigheid van D-aminozuren, H_2O_2 produceren. D-aminozuren zijn normaal gesproken niet aanwezig in de cel en daardoor biedt DAAO de mogelijkheid om in de cel op specifieke plekken H_2O_2 productie te induceren. Met dit enzym en de sensor kunnen we bepaalde situaties modelleren en verder onderzoek doen naar de rol van H_2O_2 als signaalmoleculen.

Abstract

Over the last decade, the importance of redox signalling and reactive oxygen species (ROS) for maintaining physiological signal transduction have been discovered. ROS, and in particular hydrogen peroxide (H_2O_2), have previously been seen as harmful to cells, leading to oxidative stress and disease. However, in physiological concentrations, H_2O_2 acts as a second messenger in multiple signalling pathways. Research in redox signalling requires physiological environments and requires tools that can measure and model the dynamic nature of oxidation reactions. Here, we set-up two genetic tools in different model systems, to help uncover the role of the redox environment in cells. HyPer7 is a H_2O_2 sensor, that enables visualisation of the net rate of H_2O_2 production and scavenging with subcellular resolution. We set-up and characterised HyPer7 in 3D systems, to explore the use of HyPer7 in future experiments on the importance of ROS in cell processes like polarity and differentiation. We deployed HyPer7 to visualise whether there are changes in the H_2O_2-dependent redox environment after treating cells with the anti-cancer drug 5-FU, that is suspected to induce increase ROS production in cells. However, we detect no increase in HyPer7 signal upon 5-FU treatment. Besides HyPer7, we used D-amino acid oxidase (DAAO), a genetically encoded enzyme that, in the presence of D-amino acids, can produce H_2O_2 inside cells. We set-up the DAAO system in haploid cells, where DAAO proves to be a simple way to model physiological H_2O_2 production in cells. Haploid cells are often used in genetic knock-out screens, as knock-out of only one allele is sufficient for a full knock-out phenotype. DAAO expression in haploid cells creates an opportunity to use these cells in haploid genetic knock-out screens to help discover the mechanism of redox-related cell cycle arrest. Characterisation of DAAO in haploid cells showed that there is no induction of redox-related cell cycle arrest. However, ROS-induced cell death is seen in haploid cells, and can be used in future genetic screens. All in all, HyPer7 and DAAO both are useful tools and create new opportunities for exploring redox signalling.

Introduction

Redox signalling

Redox signalling is a form of signal transduction mediated by reactions in which there is a transfer of electrons between molecules, called oxidation-reduction reactions (Forman et al., 2014). These reactions can cause oxidising or reducing modifications. Protein oxidation is the most important form of redox signalling, which can lead to differences in localisation, activity, interaction partners, and several other outcomes, and thus creates an additional layer of signal transduction regulation which can be different between tissues and cells (Sies & Jones, 2020).

In redox signalling, reactive oxygen species (ROS) play a key role. ROS is a term covering a group of molecules that are derived from oxygen, formed by redox reactions or electronic excitation. Types of ROS include hydrogen peroxide (H_2O_2), the superoxide anion ($O_2^{-\bullet}$) and the hydroxyl radical ($^{\bullet}OH$) (D'Autréaux & Toledano, 2007). ROS production happens at various locations in the cell, most importantly at the mitochondria. Adenosine triphosphate generation in the mitochondria occurs by means of a flow of electrons through the electron transport chain (ETC), resulting in the reduction of oxygen to water. During this process, electrons can be released prematurely and react with oxygen, forming $O_2^{-\bullet}$ (Holmström & Finkel, 2014). $O_2^{-\bullet}$ is an unstable molecule and dismutates spontaneously to form O_2 and H_2O_2. Superoxide dismutases (SOD) expressed in the cell can catalyse this reaction.

Mitochondria and ROS formation at the ETC has been studied extensively for half a century. However, the physiological effects of ROS generation on the rest of the cell have been studied less. Previously, it has been thought that ROS were mostly harmful, damaging molecules like DNA (Ames et al., 1993). These harmful effects occur in an 'oxidative distress' state, in which the concentration of ROS is higher than physiological levels. This higher concentration of ROS leads to unspecific oxidation of proteins, lipids and DNA, causing dysregulation in the cell and can lead to numerous diseases, like cancer. However, physiological levels of ROS result in a 'oxidative eustress' state, where ROS act as signalling molecules in specific pathways, and play a significant role in processes like cell differentiation, proliferation, or migration (Sies & Jones, 2020).

Not every ROS can directly interact with proteins and attribute to cell signalling. ROS have different chemical characteristics and can show varying reactivity to different molecules. $O_2^{-\bullet}$ ions have more reactivity towards molecules with iron-sulphur clusters, whereas H_2O_2 reacts with cysteine residues in proteins (D'Autréaux & Toledano, 2007). H_2O_2 can act on the thiol side chains (-SH) of cysteine, resulting in a reversible oxidation into a reactive sulfenic acid (-SOH). This sulfenic acid creates an ability for the protein to form disulphide bridges (-S-S-) with other cysteine residues in different domains or even different proteins (Sies & Jones, 2020). This cysteine oxidation is reversible: the cell has an extensive system that can reduce ROS itself and reverse the modifications that occur. Important enzymes in this category are peroxiredoxins and thioredoxins (Trx) for scavenging H_2O_2 and reducing oxidised cysteines, as well as SODs for dismutation of superoxide into H_2O_2 (Holmström & Finkel, 2014). Another important part of the reductive system is glutathione, a small peptide that is responsible maintaining redox homeostasis.

As ROS are reactive molecules, the question arises as to how they can reach a certain level of specificity in this process for signalling. H_2O_2 is the most important ROS in this process, as it is the most stable ROS and does not necessarily randomly oxidise molecules. Besides, the accessibility and reactivity of cysteine residues varies between different proteins, as well as within the same protein (D'Autréaux & Toledano, 2007; Forman et al., 2014). The accessibility and reactivity depend on the surrounding amino acids in the protein. The different amino acids determine the folding of a protein, and thereby the accessibility

of amino acids: cysteines on the inside of a protein are not as accessible as on the outside. The charge of the amino acids surrounding the cysteine can alter the ionisation state of the thiol group of the cysteine, and thereby the reactivity. Another reason is that H_2O_2 can be restricted to a certain location in the cell by confining the production site or by regulating the subcellular location of antioxidant enzymes that reduce H_2O_2 (Holmström & Finkel, 2014).

Redox sensors

In the past decade, several methods for visualising oxidation and redox signalling have been developed (Abo & Weerapana, 2019; Schwarzländer et al., 2016). One of the methods for visualising oxidation in the cell is by monitoring the post translational modifications that occur upon oxidation, such as the oxidation of cysteine by H_2O_2. Chemical probes have been developed to detect these modifications, and directly distinguish between the different forms of ROS responsible for the modification. Proteomic screens can show modifications that occur as a consequence of redox signalling, such as sulphenylation or sulphinylation. However, these post translational modifications have a dynamic nature, and it is difficult to analyse these modifications correctly. Besides, these methods cannot be used to provide spatiotemporal information about oxidation in the cell (Abo & Weerapana, 2019).

Another method is to visualise ROS production directly. Detection of ROS production can occur by e.g., staining live cells with a small molecule probe. Read out of these chemical probes can be luminescence, fluorescence or absorbance of electron energy (Abo & Weerapana, 2019). The downside of these small molecule probes is low sensitivity and lack of selectivity; most often they are not specific for only one ROS. To improve detection of ROS production, fluorescent protein-based redox probes have been developed, which can be genetically encoded in the cell. These genetically encoded probes can be combined with specific promoters and localisation sequences, targeting the protein to any subcellular or tissue-specific location (Pang et al., 2021). Probes are most often based on ratiometric read-outs, and thus varying expression levels between cells does not affect the results. The probes can therefore provide spatiotemporal information during live imaging, and in such way provide information on redox signalling and ROS production in the cell.

Genetically encoded fluorescent probes have been developed for multiple different systems and use different mechanisms. For example, there are probes that report on reduction systems, probes that are based on Fluorescence Resonance Energy Transfer (FRET), and probes directly measure H_2O_2. In the last category, two sensor families are best known, the roGFP2-Orp1 family, and the HyPer family (Abo & Weerapana, 2019; Pang et al., 2021). roGFP2-Orp1 sensors are based on a redox sensitive GFP, coupled to a yeast peroxidase, Orp1, making it specific for H_2O_2. HyPer probes are based on a circularly permuted YFP, attached to a H_2O_2 sensory domain of bacteria. Both probes have had multiple improvements over the last years. However, the most recent roGFP2-Tsa2ΔC_R is not suitable for mammalian systems. HyPer probes have been successfully applied to mammalian systems, but were less sensitive and pH dependent. The latest version, HyPer7, has eliminated these problems, and has been used in experiments mentioned in this report.

HyPer7 consists of a yellow fluorescent protein (YFP), integrated in a H_2O_2-sensing domain from the bacteria *Neisseria meningitidis*, the OxyR regulatory domain (Fig. 1A; (Pak et al., 2020)). The OxyR domain contains a specific cysteine residue that is selective towards H_2O_2. Readout of the probe is dependent on both oxidation by H_2O_2 as well as the speed at which HyPer7 is reduced by the reductive system. Oxidation of HyPer7 can be visualised through determining the ratio of 405nm and 488nm excitation. Upon oxidation, excitation spectra show a decrease in 405nm and an increase in 488nm (Fig.

1C). Therefore, a high 488/405 ratio denotes an oxidised probe, and a low ratio denotes a reduced probe. The emission peak of HyPer7 is located at 516 nm (Pak et al., 2020). HyPer7 can visualise H_2O_2 production in the cell, but the oxidation of HyPer7 is also dependent on the reductive system in the cell. The Trx system is responsible for reduction of HyPer7 in the cell (Pak et al., 2020), and Trx itself is also dependent on reduction by other reductive proteins, like glutathione, and cofactors like NADPH. HyPer7 is therefore in a balance between the presence of H_2O_2, and the reductive system in the cell. Oxidation could mean an increase in H_2O_2 production, but also a decrease in reductive power, or the two combined. HyPer7 makes it possible to visualise, and thereby monitor, the redox state directly through live imaging, during different processes.

Modelling H_2O_2 production in cells

As mentioned before, H_2O_2 most likely reaches a level of specificity for signalling by being restricted to a specific subcellular location, caused by localised production sites of H_2O_2 and the presence of reductive enzymes and proteins. Administering a bolus of exogenous H_2O_2 to the cells increases H_2O_2 levels throughout the cell, which prevents studying the role of the subcellular localisation of H_2O_2. To be able to model H_2O_2 production from the inside of cells, the enzyme D-amino acid oxidase (DAAO) can be used (Matlashov et al., 2014). DAAO is an enzyme that catalyses the oxygen dependent conversion of a d-amino acid into its corresponding α-keto acid, producing ammonia and H_2O_2. It is specific for D-amino acids, which are naturally not present in most mammalian cells. In humans, the DAAO gene is present, however it is only expressed at very low levels in the brain (Pollegioni et al., 2018). Here we use a catalytically more active DAAO of the yeast *Rhodotorula gracilis*. The construct of DAAO can be stably brought to expression in cell systems, and thereby can be targeted to subcellular compartments, allowing for a localised and controlled production of H_2O_2 (Matlashov et al., 2014).

Aims

The redox field is not a novel field in research; there are a myriad of papers on redox reactions, the chemical properties of ROS, and the role of mitochondria. In the last years, the amount of research in cellular environments has increased, which is necessary to put redox signalling into context and explain the essential role of H_2O_2 in cellular biology. To be able to perform such research, genetic tools have been developed. In this report, I aim to uncover more about using and optimising two novel genetic tools, to expand the current genetic toolbox available for redox signalling. With these tools, we hope to explore the role of H_2O_2 in several cellular processes. This report consists of three separate projects, researching the use of HyPer7 and DAAO.

Results

Measuring the redox environment in 3D systems using HyPer7

Previously in our lab, it has been discovered that an asymmetric distribution of H_2O_2 promotes asymmetric cell division in *C. elegans* zygotes (De Henau et al., 2020). Symmetry breaking is a primal step in processes like polarity, differentiation, or even tissue morphogenesis and development. Previous findings have also suggested a role for ROS in development (reviewed in (Hansen et al., 2020)) and tissue morphogenesis (reviewed in (Hebbar & Knust, 2021)). To further investigate the role of H_2O_2 in polarity and differentiation, HyPer7 was set-up in 3D model systems. Redox sensors have been used previously for studying development, for example in *C. elegans* or zebrafish, but not in mammalian systems. Here, we have explored the use of Madin-Darby Canine Kidney (MDCK) cysts and mouse small intestinal (MSI) organoids to set-up HyPer7 for future polarity experiments.

MDCK cells are a simple model for exploring polarity. A single MDCK cell in a matrix-like environment like Matrigel will proliferate and form a three-dimensional sphere, called a cyst (O'Brien et al., 2002). This sphere has a single round lumen, with the apical side of the cells facing the lumen, and the basal side facing outwards. A simple way of visualising this polarity is by staining the F-actin, which localises apically, and E-cadherin, which localises basolaterally (Fig. 2A). Organoids are also grown in a 3D matrix-based environment in the presence of specific growth factors (Sato & Clevers, 2013). MSI organoids show a crypt villi structure, with stem cells residing at the base of the crypt and cells differentiating up the villi. MSI organoids recapitulate the features and processes of the intestine, such as apical-basal polarity, cell differentiation and tissue morphology. The MDCK cysts are a clear and simple model for polarity, while the MSI organoids are an excellent model for more complex polarity and cell differentiation. MDCK cells and MSI organoids are mammalian model systems, and thus are relevant for translating results to human-related diseases. These models would be particularly useful for exploring redox environment using HyPer7 in processes like polarity and differentiation, but also in different cell types or even cancerous organoids. We have not been able to perform these experiments in MDCK or MSI organoids, but we have characterised HyPer7 in MDCK cells.

To measure the redox environment in different cellular compartments, we generated a plasmid containing the gene encoding for HyPer7 fused to various localisation tags using a lentiviral backbone with a hEF1 promoter (Fig. 1B). This allowed us to create stable mammalian cell lines using viral transduction. HyPer7 was localised to the cytoplasm (NES), the nucleus (NLS), the mitochondrial matrix (MLS) and the mitochondrial intermembrane space (IMS).

We used viral transduction to stably express the HyPer7 construct in MDCK cells and RPE cells, after which we grew out monoclonal cell lines. We then validated the localisation of the HyPer7 probe by examining the cells with confocal microscopy. RPE cells expressing HyPer7-NES or HyPer7-NLS show a clear cytoplasmic or nuclear localisation (Fig. 1D). MDCK cells expressing HyPer7-IMS or HyPer7-MLS, were treated with tetramethylrhodamine methyl ester perchlorate (TMRM) to stain mitochondria. TMRM and HyPer7 signal overlap (Fig. 1E), confirming the mitochondrial localisation of HyPer7 in these lines. Confirmation of the exact submitochondrial location is still needed. To validate the activity of the HyPer7-NES and -NLS constructs, a titration of H_2O_2 was performed by Daan van Soest (Fig. 1F). These validation experiments show that HyPer7 is a sensitive probe, showing increased oxidation upon exogenously added H_2O_2 at concentrations as low as 5µM for the HyPer7-NES, and from 25µM for the HyPer7-NLS. With higher concentrations of H_2O_2, the probe takes longer to be reduced again. This might be explained by depletion of reductive capacity. From these experiments it can be concluded that the

lentiviral HyPer7 construct localises correctly in mammalian cell systems and has a high sensitivity for detecting H_2O_2.
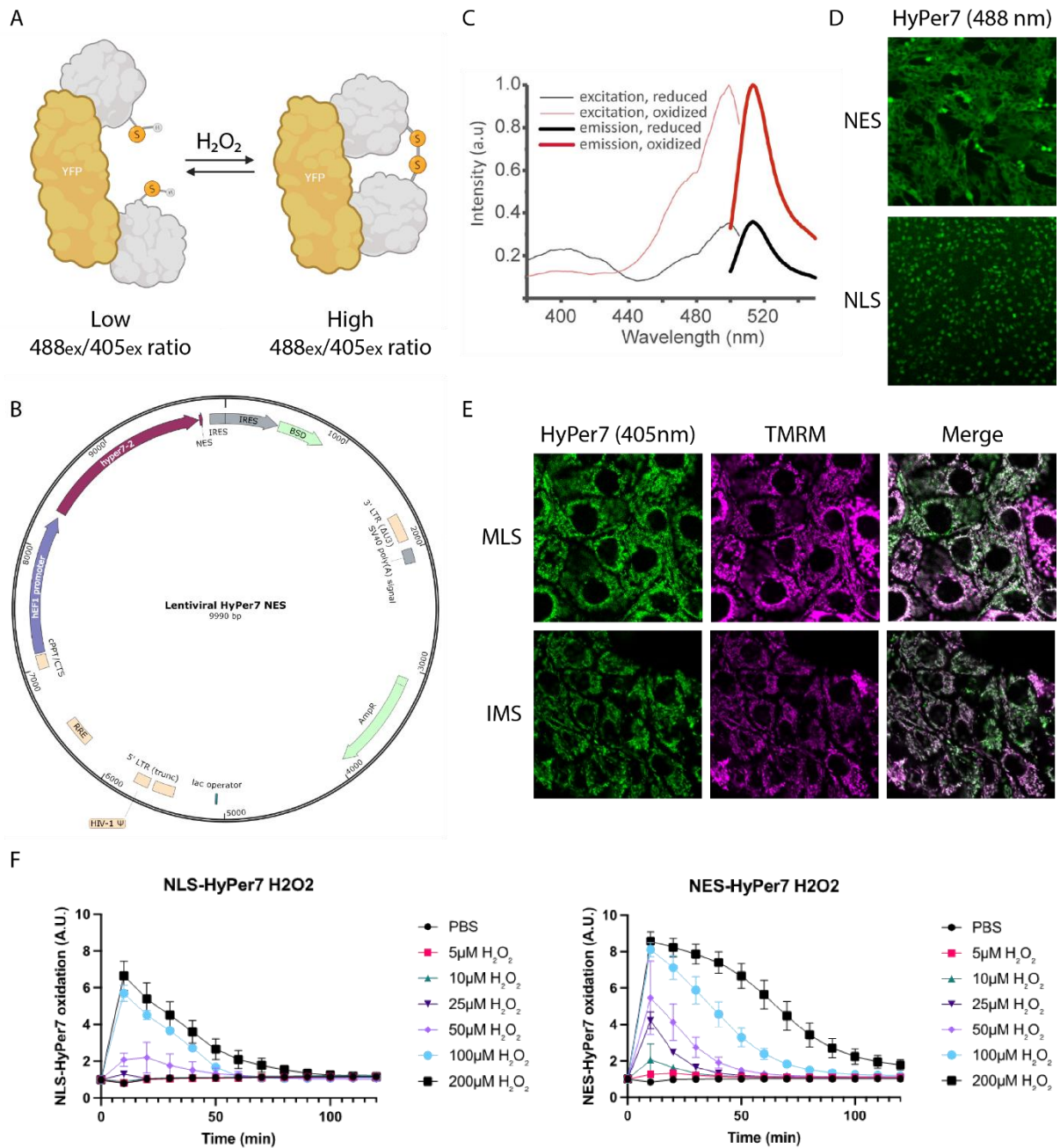

*Figure 1 – HyPer7 is a genetically encoded tool that can be used to measure H_2O_2 levels in different cellular compartments. **A** Schematic depiction of the HyPer7 protein, containing a YFP and H_2O_2 sensing domain. The probe can be oxidised in presence of H_2O_2, which results in a higher $488_{ex}/405_{ex}$ ratio. **B** The vector construct of HyPer7 with hEF1 promotor, containing a localisation tag, in this case NES, and an internal ribosomal entry site to ensure the blasticidine resistance gene to be transcribed together with HyPer7. The rest of the construct consists of genes necessary for lentiviral transduction, and an ampicillin resistance gene for transformation in bacteria. Software used for vector depiction: SnapGene Viewer. **C** HyPer7 has a different excitation spectrum in oxidised and in reduced state. The excitation maxima are at 400 and 499 nm. Emission spectra match in oxidised and reduced state, with a maximum at 516 nm. Figure from (Pak et al., 2020). **D** Localisation of HyPer7 in cytoplasm (NES) and in nucleus (NLS) in RPE cells stably expressing HyPer7-NES and -NLS. Courtesy of Daan van Soest. **E** Localisation of HyPer7 in the mitochondrial matrix (MLS) and intermembrane space (IMS) in MDCK cells. The cells have been treated with Tetramethyl rhodamine, Methyl Ester, Perchlorate (TMRM) dye, to stain active mitochondria. **F** HyPer7 is a sensitive probe and can detect different concentrations of H_2O_2. Quantification of H_2O_2 titration on RPE cells stably expressing HyPer7-NES and -NLS. Cells are given treatment after t=0. Data normalised to the ratio prior to the addition of H_2O_2. Each point represents the mean of 3 biological replicates. Courtesy of Daan van Soest.*

To test whether HyPer7 is suitable for 3D systems, we grew MDCK HyPer7 NES cysts in Matrigel for 3 days, after which we performed confocal microscopy. The cells were excited at 405nm and 488nm to be able to visualise the HyPer7 oxidation, and emission was measured. The ratio $488_{ex}/405_{ex}$ is determined during analysis (Fig. 2B). This was also done for a MSI organoid line transduced with HyPer7-NES; however, we lost the organoid line due to an infection before it could be single-cell sorted. HyPer7 is expressed stably in 3D systems and can be visualised clearly using confocal microscopy.

To see how the HyPer7 system reacts to oxidation changes in 3D systems, we performed an H_2O_2 titration. We treated the MDCK HyPer7-NES with different concentrations of H_2O_2 (Fig. 2C), starting from 250μM, because lower concentrations did not induce HyPer7 oxidation in previous experiments (data not shown). Surprisingly, HyPer7-NES does not show increased HyPer7 oxidation for concentrations lower than 1250μM H_2O_2. For 1250 and 1500 μM H_2O_2, the probe shows up until a 9-fold increase. A hypothesis for having to use higher H_2O_2 concentrations is that proteins in the Matrigel in which the cysts are grown react with the H_2O_2 added to the media. Hence, the H_2O_2 has reacted with other molecules before it can reach the cysts at concentrations lower than 1250 μM. Besides, treatment with 1500μM of H_2O_2 gives an earlier response of HyPer7, than treatment with 1250μM of H_2O_2. This substantiates the hypothesis that H_2O_2 is reacting with molecules in the medium and Matrigel. The Matrigel and medium could act as a buffer, which means that the H_2O_2 will have to interact with the molecules and therefore it takes time before the H_2O_2 reaches the cysts. A higher concentration, and therefore more H_2O_2 molecules, will decrease the amount of time it takes for the Matrigel and medium components to be saturated, and H_2O_2 is able to reach the cysts sooner. Besides, it also shows that HyPer7 can distinguish different concentrations when cells are grown in Matrigel. It seems that not all cells in the cyst oxidise at the same time: in some cells, HyPer7 is already starting to oxidise at 55 minutes, while the rest follows in the minutes after, when at 60 minutes, all the cells show high HyPer7 oxidation (Fig. 2C). Important to note is that the images were taken at an interval of 5 minutes, though H_2O_2 reacts more rapidly. This means that the oxidation of HyPer7 could be quicker than 5 minutes, but this is not visible. Overall, these results show that HyPer7 can react to H_2O_2 in 3D systems and distinguish different concentrations, although higher concentrations are needed compared to 2D cell culture.

Next, we investigated the effect of a different oxidising agent on HyPer7 in cysts. Menadione is a redox cycler and forms superoxide in a series of redox reactions (Li et al., 2019). This process will continue when oxygen is present, hence it is called redox cycling. Superoxide is very reactive and unstable, and will dismutate rapidly to H_2O_2. In this experiment, MDCK HyPer7-NES cysts were cultured for 3 days, after which they were treated and simultaneously imaged (Fig. 2D). We used two different concentrations of menadione to see if there would be a difference in HyPer7-NES oxidation. 40μM of menadione gives a 6-fold increase of HyPer7 oxidation after 40-60 minutes, while 20μM of menadione gives a 3-fold increase after 100 minutes. This indicates that a lower amount of menadione causes a delay in HyPer7 oxidation. It is good to note that HyPer7 oxidation depends on both presence of H_2O_2 and the reductive capacity of the cell at that moment. Saturation of the reductive system can explain the time difference between the two concentrations. Cysts treated with 40μM of menadione have died before the end of imaging, from 450-550 minutes after treatment. The H_2O_2 treatment shows an increase in oxidation at 20 minutes already, after which the probe is nearly completely reduced. However, around 200 minutes into imaging, the probe gets oxidised again. To further investigate what happens here, we plotted the individual cysts treated with H_2O_2 (Fig. 2E). Here it can be seen that half of the imaged cysts show a full reduction of the HyPer7-NES probe after approximately 200 minutes, while the other half of the cysts show in increase in oxidation after 200 minutes, after which the cysts lose signal and die. Interestingly, this increase in oxidation is only visible in the cysts that die. We hypothesise that the observed increase in HyPer7 oxidation might be caused by the loss of reductive
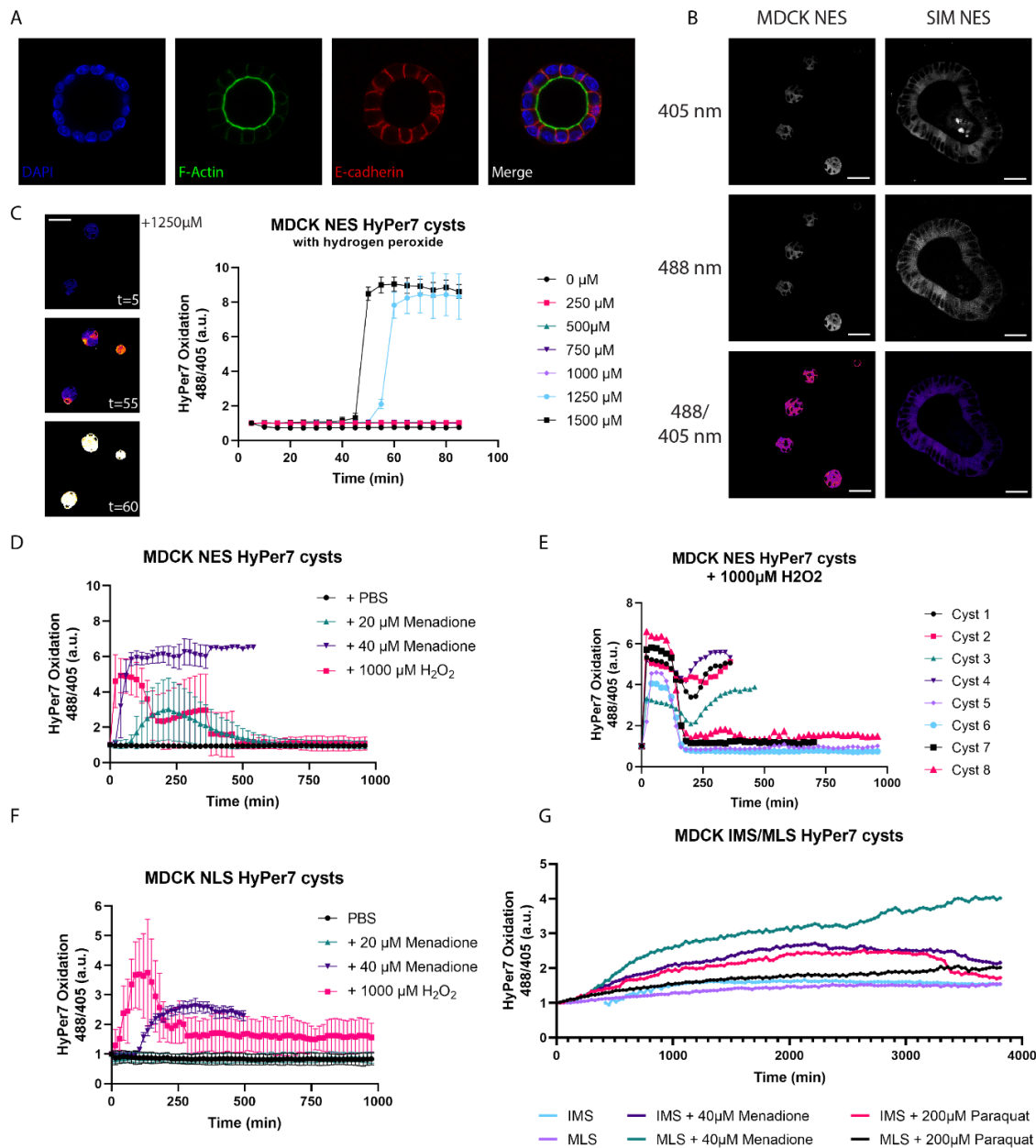
Figure 2 – HyPer7 can be used to detect H₂O₂ in different subcellular locations by live imaging. A Madin-Darby Canine Kidney (MDCK) cells can be grown in a 3D environment, forming cysts and show clear apical-basal polarity indicated by localisation of polarity markers. Cysts are fixed at day 5 and stained for DNA with DAPI, F-actin with Phalloidin (apical), and E-cadherin. B HyPer7 localises to the cytoplasm using the Nuclear Export Signal (NES) localisation tag. MDCK HyPer7 NES cysts and MSI HyPer7 NES organoids are excited at 405 and 488 nm, of which the ratio is calculated. Scalebar: 40μm. C HyPer7 is sensitive to different concentrations, as measured in MDCK HyPer7 NES cysts, and can be quantified. Images (left) of the cysts after administration of 1250μM of H₂O₂ at different timepoints. Cells are given treatment after t=0. For quantification (right), each point represents the mean of 3 cysts, and calculated standard deviation. Data normalised to the ratio prior to the addition of H₂O₂. N=1, T: minutes, Scalebar: 40μm. D HyPer7 in the cytoplasm can detect oxidation changes by H₂O₂ and menadione. Quantification of MDCK HyPer7 NES cysts. Cells are given mentioned treatment after t=0. Data normalised to the ratio prior to the addition of treatment. End of the line indicates that the cysts have died. Each point represents the mean of 8 cysts, with the standard deviation. N=1. E Quantification plot of the separate MDCK NES HyPer7 cysts treated with 1000μM of H₂O₂, of which the mean is depicted in figure 2D. End of the line indicates that the cysts have died. F HyPer7 in the nucleus with the Nuclear Localisation Signal (NLS) can detect oxidation changes by H₂O₂ and menadione. Quantification of MDCK HyPer7 NLS cysts. Cells are given mentioned treatment after t=0. Data normalised to the ratio prior to the addition of treatment. End of the line indicates that the cysts have died. Each point represents the mean of 6 cysts, with the standard deviation. N=1. G HyPer7 can detect oxidation changes in different compartments of the mitochondria. Quantification of MDCK HyPer7 IMS and MLS cysts. Cells are given mentioned treatment after t=0. Data normalised to the ratio prior to the addition of H₂O₂. Each point represents 1 cyst, N=1. For IMS (cyan), there was no signal before t=420, so data is normalised to t=420.

potential in dying cells. The amount of HyPer7 oxidation varies between cysts and experiments. This might be since not all wells contain the exact same amount of medium or Matrigel, and that the read-out of HyPer7 oxidation is therefore varying in different experiments or even different wells.

The same experiment was also performed in MDCK HyPer7-NLS cysts, to see whether H_2O_2 would also be able to reach the nucleus after these treatments (Fig. 2F). As can be seen in the figure, redox changes after treatment with 20μM of menadione are not detected in the nucleus. 40μM menadione shows increased nuclear oxidation, however it is delayed and decreased compared to the cytoplasmic HyPer7. H_2O_2 treatment also shows decreased induction of NLS-HyPer7 oxidation compared to NES-HyPer7. These results show that the H_2O_2 produced by menadione, or administered exogenously, are reduced before it reaches the nucleus, and that the reductive capacity in the nucleus is high. A higher concentration of menadione results in more HyPer7 oxidation, indicating a loss in reductive power in or around the nucleus. It might also indicate that menadione does not produce H_2O_2 in the nucleus, as ratios of HyPer7 oxidation in the cytoplasm (Fig. 2D) are higher. To conclude, these experiments show that the HyPer7-NES probe in cysts can visualise changes in redox environment upon different concentrations of menadione, and that HyPer7 can detect minor redox differences between different compartments in the cell.

Besides the cytoplasmic and nuclear HyPer7, we also wanted to test HyPer7 located in the mitochondrial intermembrane space and matrix. We imaged the HyPer7-IMS and -MLS cysts over longer periods of time, with or without treatment of oxidising agents, to see whether there are differences over time in the development of the cysts. We used menadione, also used in the previous experiment, and paraquat, a well-known complex I redox cycler. For paraquat it is known that it induces superoxide formation in the mitochondrial matrix (Cochemé & Murphy, 2008); for menadione it is not clear in which cellular compartments this mostly happens.

For this experiment, we imaged the cysts for a longer amount of time, up until 60 hours (Fig. 2G). The probe remained stable throughout the entire time, which shows imaging with HyPer7 in the cells can be performed for longer amounts of time. It seems that the oxidation levels for the untreated MDCK HyPer7-IMS and -MLS slightly increase over time, but this is no substantial change compared to the treated cysts. Treatment with paraquat seems to give more oxidation in the intermembrane space than in the matrix. Menadione treated cells in general show more oxidation than paraquat, but here oxidation is higher in the matrix than the intermembrane space. This is a rather surprising find, as paraquat creates superoxide in the matrix, not in the intermembrane space. This could mean that somewhere between the superoxide production and the H_2O_2 formation, there is an unknown step, that also involves relocation to the intermembrane space. For menadione, it is not entirely known where most superoxide production takes place. While we cannot find out exactly why paraquat gives lower peroxide production in the matrix than in the intermembrane space, we can conclude that the HyPer7 probe is able to visualise minor changes in peroxide production between two neighbouring compartments. If results were similar between both IMS and MLS HyPer7, it could have been due to overlap in localisation.

Overall, these results show that HyPer7 is suitable for use in 3D systems; cells express HyPer7 stably, and the cells can be imaged for days. On the downside, HyPer7 shows a lower sensitivity than in 2D set-ups, due to the presence of a matrix-like environment with which H_2O_2 can react. By expressing the probe in different cellular compartments, the ever-changing redox environment can be detected and visualised, even within mitochondria.

Determining whether 5-FU treatment alters the redox environment in RPE cells

5-fluorouracil (5-FU) is a chemotherapeutic drug, used as treatment for a range of cancers. Treatment with 5-FU results in problems with DNA and RNA synthesis, by inhibiting specific nucleotide synthetic enzymes, or by incorporating wrong nucleotides during DNA or RNA synthesis (Longley et al., 2003). This is particularly disadvantageous for cells that replicate rapidly like cancer cells, which use the DNA and RNA synthesis to a great extent. To determine the consequences of 5-FU treatment on DNA, the Cuppen lab performed a mutational signature analysis (Christensen et al., 2019). The mutational signature found after treating organoids with 5-FU was very similar to COSMIC signature 17, characterised by T>G mutations. This signature is not immediately related to ROS. However, ROS have been known to cause DNA damage, which happens among others through oxidation of guanines to 8-oxo-G. Presence of an 8-oxo-G in DNA can lead to a mismatch in replication, causing a C>A mutation. However, guanines in the nucleotide pool in the cytoplasm can also be oxidised to 8-oxo-G. When 8-oxo-G is then incorporated in the DNA, it is mismatched with an adenosine, leading to a T>G mutation, as found in the mutational analysis (Christensen et al., 2019). This led to the hypothesis that 5-FU might promote ROS production and that this causes the mutational signature, but the mechanism is not clear. To be able to visualise ROS production after 5-FU treatment, we use HyPer7, which is able to detect increased H_2O_2 levels as well as a decreased Trx reductive system. In that way, production of ROS besides H_2O_2 that are part of the Trx reduction system, can also be detected.

For these experiments we used RPE cells, stably expressing HyPer7-NES and –NLS, so that the entire cell is covered by these probes. We treated cells with different concentrations of 5-FU, ranging from 0-250µM, for approximately 18 hours (Fig. 3A-B), or 4 hours (Fig. 3C). These concentrations are different than the concentrations used in (Christensen et al., 2019), because 5-FU responds differently in different cell types. After treatment, we washed the cells using PBS containing N-Ethylmaleimide (NEM), so free thiols are alkylated and the oxidation state of HyPer7 is fixed. Then, we trypsinised the cells and fixed them with paraformaldehyde. The samples were analysed using flow cytometry, gating for high expression of HyPer7, after which the ratio of HyPer7 is determined. Treatment with 5-FU did not have any significant effect on the HyPer7 oxidation in neither NES nor NLS located HyPer7, or for longer and shorter amounts of time treated. Treatment with H_2O_2 as a positive control shows differences between adding H_2O_2 15 or 30 minutes before fixation. 30 minutes after adding H_2O_2, the signal has decreased slightly, probably because the cells have had more time to clear H_2O_2 and reduce the HyPer7 probe. Overall, these experiments show that there is no H_2O_2 production after treatment with 5-FU.

Fixing cells and flow cytometry analysis only report on HyPer7 oxidation at a certain timepoint. To see what happens over time after 5-FU treatment, we tested this setup with live imaging overnight. RPE HyPer7-NES and –NLS cells were imaged in the Zeiss Cell Observer upon treatment after imaging the baseline (Fig. 3D). 5-FU is dissolved in DMSO, so DMSO was taken along as a negative control. H_2O_2 treatment served as a positive control and indeed shows an increase in oxidation at the start, after which the probe is reduced again in 100-150 minutes. To conclude, in this experiment, HyPer7 showed no H_2O_2 production in either cytoplasm or nucleus after treating with 5-FU.

All in all, RPE-HyPer7 cells show no increased oxidation in the cells, for either flow cytometry analysed, or live-imaged cells. Different concentrations and length of treatments also show no differences in a timeframe of 1 to 2 days. 5-FU treatment gives no ROS production detectable to HyPer7. Whether 5-FU treatments might give ROS production that is not related to the Trx system, or whether reduction systems are depleted are not clear.
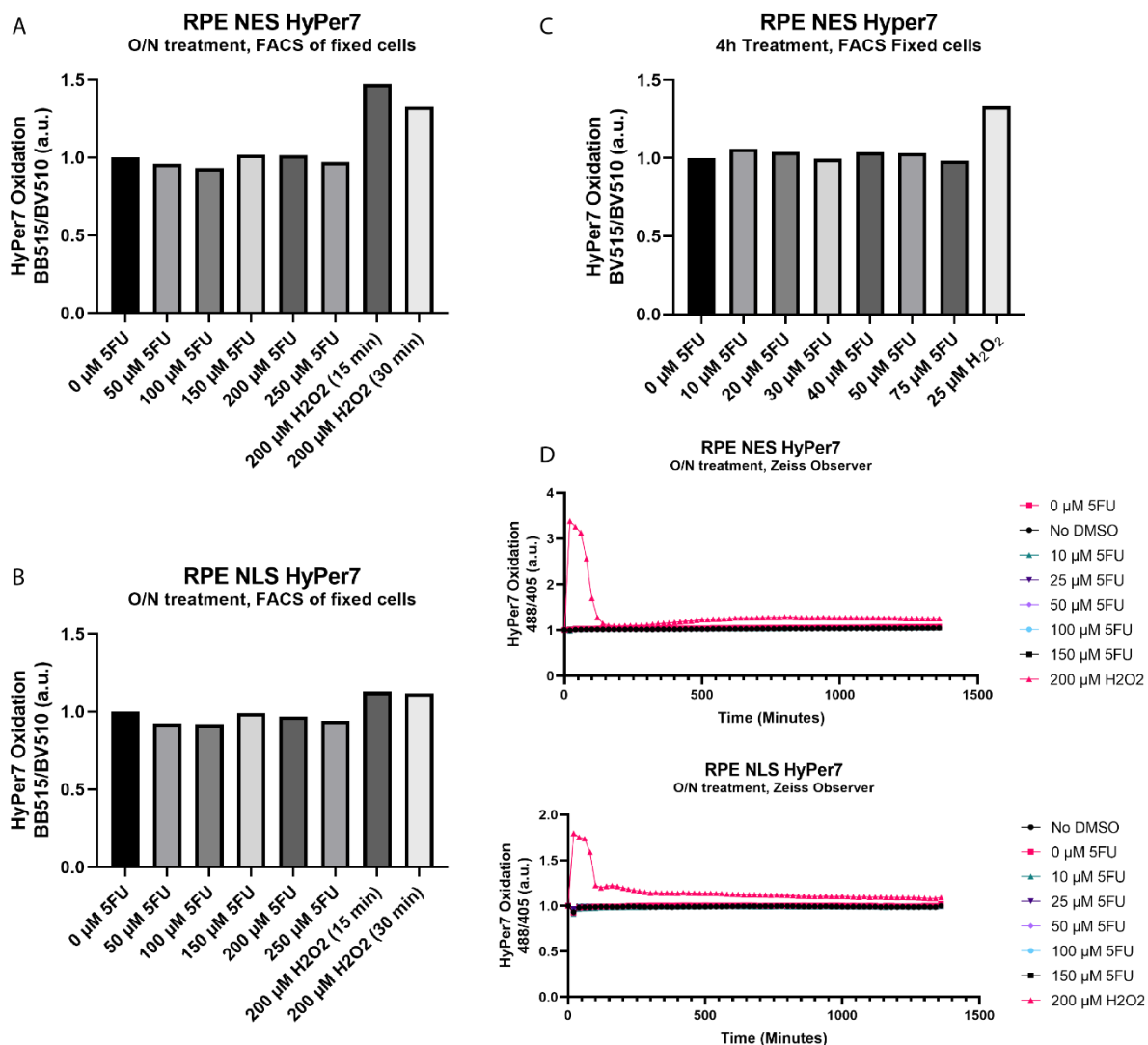
*Figure 3 - Using HyPer7 in RPE cells to detect possible H_2O_2 formation after 5-FU treatment shows no changes in HyPer7 oxidation. **A** RPE cells stably expressing HyPer7-NES have been treated with the mentioned concentrations of 5-FU for approximately 18 hours, before fixation. For H_2O_2 treated cells, peroxide was added 15 or 30 minutes prior to fixation. During fixation, PBS containing N-Ethylmaleimide (NEM) was used to fix the oxidation state of HyPer7, and after, samples were analysed by flow cytometry. Bars show the ratio of the geometric mean of BB515/BV510 in 10.000 cells. **B** RPE HyPer7-NLS cells have been treated with the mentioned concentrations of 5-FU for approximately 18 hours, before fixation. For H_2O_2 treated cells, peroxide was added 15 or 30 minutes prior to fixation. During fixation, PBS containing NEM was used to fix the oxidation state of HyPer7, and after, samples were analysed by flow cytometry. Bars show the ratio of the geometric mean of BB515/BV510 in 10.000 cells. **C** RPE HyPer7-NES cells have been treated with the mentioned concentrations of 5-FU for 4 hours, before fixation. For H_2O_2 treated cells, treatment was 15 minutes before fixation. During fixation, PBS containing NEM was used to fix the oxidation state of HyPer7, and after, samples were analysed by flow cytometry. Bars show the ratio of the geometric mean of BB515/BV510 in 5.000 cells. **D** RPE HyPer7-NES (top) and –NLS (bottom) cells have been live imaged using the Zeiss Cell Observer microscope. Cells are given mentioned treatment after t=0. Data normalised to the ratio prior to the addition of treatment. Each point represents the mean of the cells in field of view (approx.. 250 cells). N=1.*

Exploring redox-dependent cell cycle arrest in haploid cells for future genetic screens

Experiments in our lab have shown that following treatment of RPE cells with DAAO in the nucleus with different concentrations of D-alanine, cells stop growing and show a cell cycle arrest in the 4N stage (data not shown). DAAO was attached to histone 2B (H2B) in the nucleus, and to TOM20, a mitochondrial tag, localising at the outside of the mitochondria. Following treatment of these two cell lines with 5 or 10 mM of D-alanine for 48 hours, the cells were analysed with flow cytometry and an increase of the 4N peak for H2B-DAAO cell lines is visible. To be able to uncover a mechanism as to how ROS could be able to induce a cell arrest, a genetic screen could be performed. Classic genetics, applying targeted mutations to genes is a very powerful method for uncovering underlying mechanisms. However, generating a full knock-out of both alleles in diploid cells is inefficient. To solve this problem (near) haploid cell lines are frequently being used for genetic knock-out screens (Carette et al., 2009). Since haploid cells only contain a single copy of every gene, this method is more efficient and powerful. In such screens, CRISPR/Cas can be used to knock out specific genes. To be able to conduct haploid genetic screens for the mechanism behind ROS-induced cell cycle arrest, we made HAP1-DAAO cell lines, using lentiviral transduction, for both TOM20 and H2B-DAAO. HAP1 cells are a near haploid cell line, derived from the near haploid KBM-7 Chronic Myeloid Leukaemia cells. If these cells show a similar phenotype, i.e. redox induced cell cycle arrest, a genetic screen can be performed in which cells that grow out after D-alanine treatment have been hit by guide RNA targeting a gene important in cell cycle arrest.

To determine whether DAAO works in the HAP1 cells, we treated the HAP1 TOM20-DAAO and H2B-DAAO cells for 48 hours with different concentrations of D-alanine, to induce H_2O_2 production. We performed a crystal violet viability assay (Fig. 4A). DAAO-induced H_2O_2 induces loss of cell viability in H2B-DAAO expressing cells in a [D-alanine] dependent manner. L-alanine serves as a negative control, and shows similar cell density to untreated cells. For TOM20-DAAO HAP1 cells, the cells seem fuller from the start, most likely due to an error in cell counting, or perhaps due to faster replication. Most loss of viability was observed at 40mM of D-alanine. Treatment with D-alanine at concentrations lower than 40mM does not induce as much loss in viability in TOM20-DAAO cells as in H2B-DAAO cells. It is however not easy to compare the two because of different cell densities. A flow-cytometry-based Propidium Iodide (PI) exclusion assay was used to determine whether loss of viability was accompanied by increased cell death. Cells were treated with different concentrations of D-alanine, after which the cells were stained with PI. PI is a membrane impermeant dye, meaning it can only stain dead cells, which can be easily quantified using flow cytometry. H2B-DAAO cells show an increasing amount of cell death with an increasing amount of D-alanine, and TOM20-DAAO cells show small or no differences in cell death, up until 40 mM of D-alanine, when more than half of the cells are dead. These results resemble the results from the crystal violet staining, and are also similar to the results we see when treating RPE-DAAO cells with D-alanine (data not shown). These results show that DAAO is functioning in HAP1 cells and that DAAO in HAP1 cells induce a redox-dependent cell death.

Next, a flow cytometry cell cycle profile was performed to assess whether DAAO-induced H_2O_2 induces a similar cell cycle arrest as to what has been seen in RPE cells. HAP1-DAAO cells were treated with different amounts of D-alanine for 48 hours, after which the cells are fixed and stained with PI. In a cell cycle profile, the amount of DNA in the is quantified, and cells that have replicated DNA, in G2 and M phase (for haploid cells: 2N), can be distinguished from cells in G1 phase (for haploid cells: 1N) by two different peaks in de flow cytometry histogram. After treatment of H2B-DAAO or TOM20-DAAO HAP1 cells with D-alanine, there seems to be no increase in the 2N-containing cells (Fig. 4C). For the TOM20-DAAO cells, there does seem to be a slight increase in 2N cells at 20 and 40 mM of D-alanine. However,

after these treatments, more cell death has occurred, and samples contained less cells. From this experiment we conclude that there seems to be no cell cycle arrest when treating cells with D-alanine for neither TOM20-DAAO nor H2B-DAAO in HAP1 cells. However, the redox-dependent cell death due to DAAO induced H_2O_2 can be of use in a haploid genetic screen.
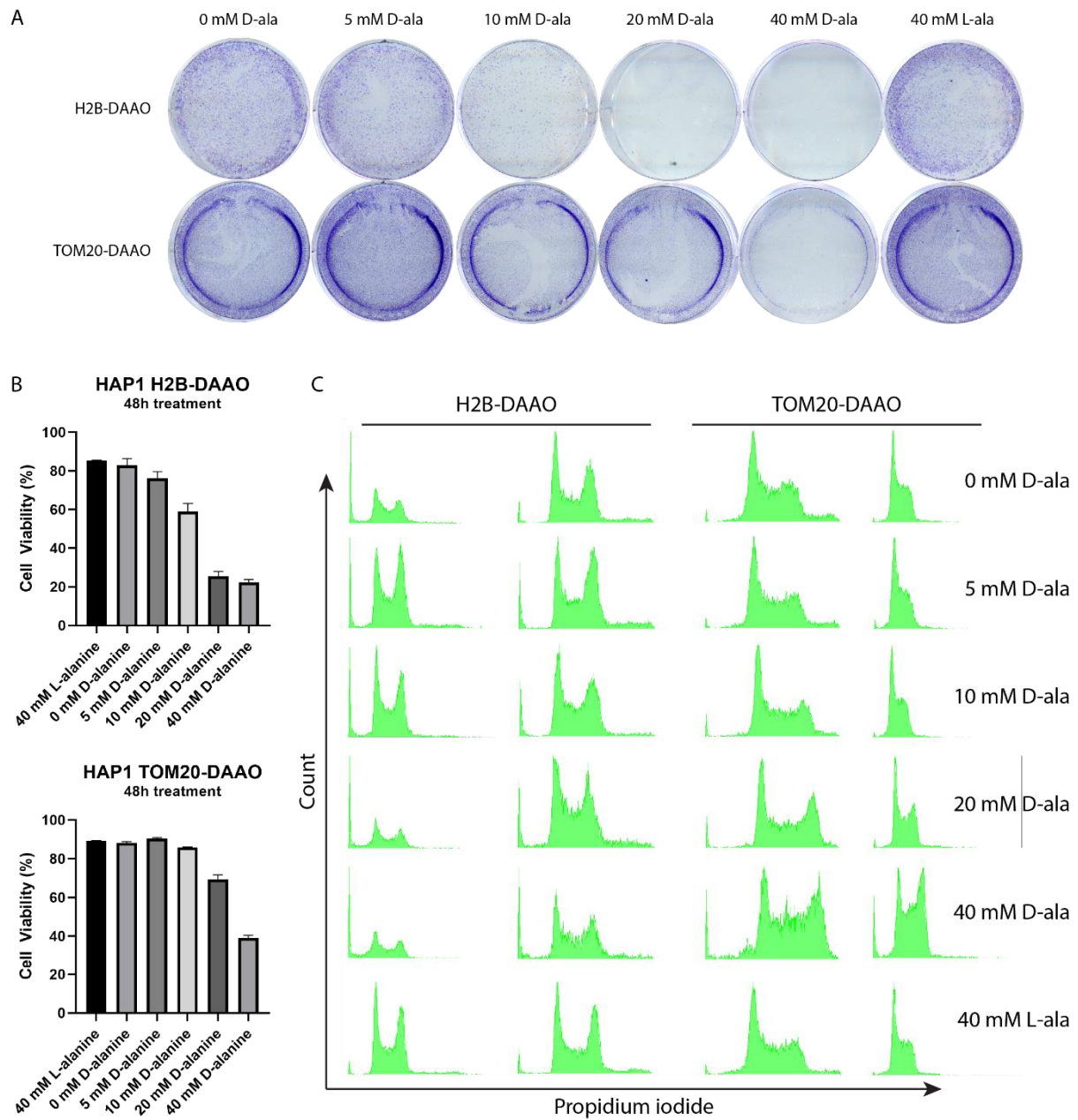

*Figure 4 - HAP1 cells expressing H2B-DAAO or TOM20-DAAO show increasing amounts of cell death when treated with increasing amounts of D-alanine, but show no cell cycle arrest. **A** Crystal Violet assay of TOM20-DAAO and H2B-DAAO HAP1 cells. Cells were treated for 48 hours with mentioned treatments, after which the cells were fixed and stained with crystal violet to show adherent cells. L-alanine serves as a negative control for D-alanine treatments. **B** Propidium Iodide (PI) exclusion assay of TOM20-DAAO and H2B-DAAO HAP1 cells. Cells were treated for 48 hours with mentioned treatments, after which cells were stained with PI. For each condition, two technical replicates were taken along. Cells were analysed using flow cytometry, calculating the ratio of cells containing PI (dead cells) versus the total number of cells quantified. **C** Cell cycle profile of TOM20-DAAO and H2B-DAAO HAP1 cells. Cells were treated for 48 hours with mentioned treatments, after which the cells were fixed and stained with PI for quantifying DNA content. Two rows per cell line show technical duplicates.*

Discussion

Here, we set-up HyPer7 in 3D systems like MDCK cysts and MSI organoids, to explore the use of HyPer7 for future experiments on the importance of ROS in polarity and differentiation. HyPer7 can be imaged over longer periods of time in 3D systems, and can visualise differences between cellular compartments Besides, we used HyPer7 to detect changes in the redox environment after treating cells with the anti-cancer drug 5-FU. However, there seemed to be no changes after 5-FU treatment. Lastly, we set-up the DAAO system in HAP1 cells so we can perform a haploid genetic screen. Local production of H_2O_2 caused no cell cycle arrest in HAP1 cells, but there was an increasing amount of cell death with higher levels of H_2O_2 production.

Measuring the redox environment in 3D systems using HyPer7

HyPer7 has not been previously used in mammalian 3D systems. Previous studies have used small molecule dyes in zebrafish and Drosophila to measure the oxidising milieu (Hunter et al., 2018), or created transgenic animals like *C. elegans* with roGFP2-Tsa2ΔC$_R$ (De Henau et al., 2020), or mice with a cpYFP sensor for superoxide (Wang et al., 2008). Also prior versions of the HyPer family have been used in many different cell systems and organisms (reviewed in (Bilan & Belousov, 2016)). However, the use of H_2O_2 sensors like HyPer7 in 3D mammalian cell culture systems such as MDCK or organoids, has not been previously reported. HyPer7 is not more sensitive than the most recent GFP probe, roGFP2-Tsa2ΔC$_R$ (Kritsiligkou et al., 2021). The problem is that roGFP2-Tsa2ΔC$_R$ is not suitable for mammalian systems, and sensors might respond differently in other cells. Also, HyPer7 proves to be less sensitive to smaller changes in redox environment, because HyPer7 can be very quickly reduced (Kritsiligkou et al., 2021). This might mean that smaller varieties in concentration of H_2O_2 in processes might not be registered by the probe. Here, we show that HyPer7 is suitable for 3D systems and show that it can be used to monitor cells and their redox environment for extended periods of time, but we still have to extend the repertoire of experiments in physiological processes.

HyPer7 located in the mitochondrial matrix and intermembrane space can help give insight into H_2O_2 production at the electron transport chain. ROS production at the ETC occurs by leakage of electrons at complex I, II or III, leading to reduction of oxygen to superoxide (Nolfi-Donegan et al., 2020). Most of this superoxide production happens in the matrix, and some in the intermembrane space. SOD1 and 2, present in the intermembrane space and matrix, respectively, can dismutate superoxide to H_2O_2. Research on mitochondrial ROS production has already been performed by the lab that produced HyPer7 (Pak et al., 2020). Inhibition of complex I at the ETC resulted an increased HyPer7 oxidation the matrix, but not in the IMS and cytosol. This adds to the knowledge that is already there on mitochondrial ROS production and that mitochondria have a high reductive capacity (Mailloux, 2021). Research on the topology of H_2O_2 production between matrix and intermembrane space is not abundant. We had an interesting finding when we used paraquat with IMS and MLS-HyPer7. Paraquat is a complex I redox cycler and it is thought to only produce superoxide at the matrix side (Cochemé & Murphy, 2008). Surprisingly, we found that paraquat seemed to give more HyPer7 oxidation in the intermembrane space, than in the matrix. Good to note is that the response of HyPer7 is based on both the production of H_2O_2, as well as the reductive system and its velocity in reducing HyPer7. It could be that there is ROS leakage from the matrix to the intermembrane space, and that the reductive capacity is lower in the IMS and therefore giving higher HyPer7 oxidation in the IMS(Hu et al., 2008). Superoxide is dismutated rapidly by SODs to H_2O_2, and perhaps H_2O_2 is transported to the IMS. It could be useful to combine Hyper7 with a TOM20 localisation tag outside the mitochondria, to see whether there is ROS leakage to

the cytosol, or if all ROS is reduced before being able to exit the mitochondria. For menadione, a specific location of superoxide production was not known, however it seems that HyPer7 oxidation in the matrix upon menadione treatment is higher than in the intermembrane space. Next to that, it seems that menadione gives higher HyPer7 ratios in the cytoplasm than in the mitochondria. This could mean that redox cycling of menadione happens more in the cytoplasm, but as this result comes from two separate experiments, we are not certain. All in all, HyPer7 does prove to be a sensitive probe, and can help uncover H_2O_2 gradients in smaller compartments, like mitochondria.

There are however some limitations to using HyPer7 in 3D systems with this experimental setup. Administering a bolus of exogenous H_2O_2 seems not so effective in 3D systems, due to the matrix-environment in which the cells are grown. It also seems that there is lot of variation in HyPer7 ratios between experiments, even though the same concentration is added. Factors that weigh in are, the density of the cysts seeded, number of days after plating the cysts, and the amount of medium or Matrigel present in the wells. This could also be resolved by using HyPer7 alongside DAAO, to model various levels of H_2O_2. This has also been performed in (Pak et al., 2020). Another problem is that for the experiments with HyPer7 in the mitochondria, signal was low and difficult to detect. Differences in the ratios in mitochondria are not comparable to the differences in ratios of HyPer7 in the cytoplasm or nucleus. This might be since mitochondria are an oxidative environment, and the probe is saturated more quickly. Besides, the mitochondria are smaller compartments than nuclei or the cytoplasm, and so the average signal can be lower. For properly comparing different experiments and different localisations of HyPer7, a background subtraction needs to be taken along to only calculate ratios in the specific areas where HyPer7 is present. Also, when imaging cysts or organoids with HyPer7, it is best to use confocal microscopy. Cysts and organoids grown in a 3D environment are not directly on the bottom of a well. Confocal microscopy is better suited in 3D set-ups than regular fluorescence microscopy (data not shown) and achieves higher resolution for imaging subcellular compartments. For quantifications of larger groups of 2D cells, it suffices to use a non-confocal microscope.

3D systems are excellent models for polarity and differentiation. MDCK cells show very clear apical-basal polarity, and form 1 round lumen. Preliminary data has shown that scavenging of ROS in MDCK cysts, leads to formation of more multiple (data not shown), indicating a form of disrupted polarity. Here, we have set-up a MDCK system with HyPer7 for four different localisations, NES, NLS, MLS and IMS. Imaging the cysts with HyPer7 over longer periods of time at high resolution could be very useful for exploring whether redox signalling affects polarity in mammalian systems. It might be possible to visualise physiological differences, like a specific relocalisation of H_2O_2 production to a side of the cell, important for the cyst morphology. For MSI organoids, it is still necessary to find a suitable protocol for lentiviral transduction and single cell sorting the organoids, as not all cells in the organoid are hit by transduction. When this does succeed, polarity experiments can be expanded even further, looking for differences in crypts and villi, or visualising redox differences between different cell types, as well as during the process of differentiation. An interesting novel approach, by co-culturing HyPer7 transduced cells with different localisation tags, can be of use in future experiments (Secilmis et al., 2021). In this case, we can measure redox signalling in different compartments and compare them to each other, comparing different levels of ROS or the reductive capacity.

Determining whether 5-FU treatment alters the redox environment in RPE cells

5-FU treatment of organoids causes a mutational signature, characterised by T>G mutations. This signature has been proposed to be connected to the presence of 8-oxo-G nucleotides in the nucleotide pool (Christensen et al., 2019). To investigate whether ROS, and most importantly H_2O_2 would be

responsible for these mutations, we used HyPer7 to see if there are changes in the H_2O_2-dependent redox environment, both in the cytoplasm and the nucleus. We found that there is no change in the redox environment, when given 5-FU treatment to RPE cells with HyPer7. ROS and oxidative stress have been linked to 5-FU treatment (Focaccetti et al., 2015; Güçlü et al., 2018; Koçer & Nazıroğlu, 2013; Mavrikou et al., 2019). These studies have shown an increase of lipid peroxidation, increased levels of reductive enzymes and proteins, detection of superoxide, or increased levels of ROS. Even though 5-FU treatment and ROS production are correlated according to literature, in our experiments, HyPer7 does not show a change in redox environment. While HyPer7 specifically measures H_2O_2, changes in superoxide production should be picked up as superoxide is quickly transformed to H_2O_2. An increase or decrease in activity of the reductive systems of Trx can also be detected by HyPer7.

In the studies mentioned before, samples came from either a patient group that received 5-FU as a chemotherapy, or from cell lines with multiple and longer rounds of 5-FU treatment. A different approach in 5-FU treatment could have an effect on ROS production and the possible mutations in the nucleotide pool due to ROS, however even with live imaging HyPer7 did not detect oxidation in either cytoplasm or nucleus. Live imaging seems to be more sensitive than flow cytometry analysis, as ratios are almost 3-fold higher for live imaging. For either method, the settings still need to be optimised, and background signal must be considered. Besides, the T>G mutations have been found in 5-FU treated organoids and in patient-derived material of patient treated with 5-FU (Christensen et al., 2019). To be sure if this same mutational signature is also present in the used RPE cells upon 5-FU treatment, a mutational analysis on these cells must be performed. It might be that the observed 5-FU induced ROS and associated mutational signature is only present in tumour cells, for instance due to loss of p53.

Theories that might fit with the scenario where there is no increase in H_2O_2 visible, despite reported increases in superoxide and T>G mutations might be that 5-FU in some way inhibits 8-oxo-G repair proteins and physiological levels of ROS are responsible for nucleotide oxidation, or that the superoxide dismutases, responsible for transforming superoxide into H_2O_2, are inhibited. In testing these hypotheses, together with a different approach in 5-FU treatment, HyPer7 might still be of use to visualise any H_2O_2-dependent redox changes.

Not only 5-FU as a chemotherapeutic is correlated with induction of ROS, but many other chemotherapeutics induce ROS. High levels of H_2O_2 can induce oxidative stress, where DNA damage occurs and signalling processes are disrupted. The exact role of ROS in cancer chemotherapy has been studied, but using HyPer7 to study the dynamics of ROS in cancer can attribute to the existing knowledge (Yang et al., 2018).

Exploring redox-dependent cell cycle arrest in haploid cells for future genetic screens

The HAP1 cell line is a derivative of the KBM7 near-haploid human cell line from a patient with chronic myelogenous leukaemia (Carette et al., 2011). In order to perform haploid CRISPR/Cas9 dependent genetic knock-out screens aimed at understanding subcellular H_2O_2-dependent cell cycle arrest, we made HAP1-DAAO cell lines. The HAP1-DAAO cells show no cell cycle arrest after treatment with D-alanine, but they do show an increased cell death with higher concentrations of D-alanine, similar to RPE-DAAO cells.

Haploid cells themselves are not very stable, and culturing them can result in an increase of diploid cells over time (Beigl et al., 2020). Stability of the cell line can be prolonged by monoclonal outgrowth of a

single HAP1 cell, which we performed to ensure longer stability of the cell line. Besides, haploid cells are limited in proliferation by upregulation of p53 (Olbrich et al., 2017), even without DAAO-induced H_2O_2. When administering D-alanine, the amount of cell death increases, indicating that this cell death is H_2O_2 induced. ROS-induced cell death is seen in many different processes, also with chemotherapy. The exact mechanism of this cell death can be discovered with a haploid genetic screen, so the exact proteins that are essential in this cell death can be uncovered. Important to note, is that HAP1 cells are derived from a cancerous cell line, most likely carrying mutations that are in favour of proliferation. These mutations can also have effect on cell cycle arrest and cell death programs, which would make it difficult to research.

Because DAAO and D-amino acids are not present in most mammalian tissues, DAAO is a simple tool for modelling H_2O_2 production. Controlling this H_2O_2 production gives the power to change the redox state in specific subcellular location. DAAO has been set-up in the mitochondria, to perturb the physiological oxidation state in the mitochondria (Stein et al., 2018), or in the nucleus, to observe changes in the reduction system (Halvey et al., 2007). DAAO has also been used in combination with HyPer (Bogdanova et al., 2017; Pak et al., 2020). Together with using DAAO in haploid cells, DAAO has proved to be a helpful and effective tool in modelling H_2O_2 production and thereby attributing to research on redox signalling.

Redox signalling is an important part of several signalling pathways in cells. Research in redox signalling requires physiological environments and requires tools that can manage and model the dynamic nature of the chemical reactions involved. HyPer7 and DAAO are two genetic tools that can be very useful in redox research. We used HyPer7 in two different experimental set-ups, where HyPer7 proves to be a sensitive and stable sensor in mammalian 3D cell lines such as MDCK cells and MSI organoids. Different localisation tags provide information about the spatiotemporal response of the H_2O_2-dependent redox environment in various settings. HyPer7 shows no changes in redox environment after 5-FU treatment, but could be used with other chemotherapeutics, so that the role of ROS in signalling can be further uncovered. We also show the use DAAO in haploid cells, where DAAO proves to be a simple way to model physiological H_2O_2 production in cells. HyPer7 and DAAO both are useful tools in the genetic toolbox for exploring redox signalling.

Methods

Cell culture

MDCK cells were provided by the Gloerich group (UMC Utrecht). MDCK cells were cultured in Dulbecco's Modified Eagle's Medium (DMEM), low glucose (Sigma Aldrich D5523), supplemented with 10% foetal bovine serum (FBS, Bodinco) and 1% penicillin/streptomycin (Sigma Aldrich). HEK293T cells were cultured in DMEM low glucose (Sigma Aldrich), supplemented with 10% heat-inactivated FBS and 1% Penicillin/Streptomycin. RPE^{Tert} cells were cultured in DMEM/F-12 high-glucose (Gibco) supplemented with 10% heat-inactivated FBS and 1% Penicillin-Streptomycin. HAP1 cells were provided by the Zwartkruis group (UMC Utrecht). HAP1 cells were cultured in Iscove's Modified Dulbecco's Medium (Gibco), supplemented with 10% heat-inactivated FBS and 1% Penicillin/Streptomycin. All cell types were cultured at 37°C under a 6% CO_2 atmosphere.

MDCK cyst culture

An 80% full plate of MDCK cells were split 1:20 the day before to improve number of single cells after trypsinisation. An 8-well Lab-Tek II chamber slide (Thermo Scientific) was coated with Matrigel Matrix (Corning), diluted to 3.3mg/ml with serum-free MDCK culture medium. MDCK cells were trypsinised, counted and per well, $1.6x10^4$ MDCK cells were seeded in 400 µl serum-free cell culture medium supplemented with 3.3mg/ml Matrigel. 250µl of cell culture medium with FBS was added after Matrigel solidified, and replaced every 2-3 days upon fixation (5 days) or live imaging (2 or 3 days). Cysts were cultured at 37°C under a 6% CO_2 atmosphere.

Organoid culture

Small intestinal mouse organoids were a gift from the Snippert group (UMC Utrecht). Organoids were cultured in Basement Membrane Extract (BME; Bio-Techne) droplets with culture media that was refreshed every 2-3 days. The media composition for ENR is as follows: DMEM/F12 (Gibco) supplemented with 1% Penicillin/Streptomycin (Sigma-Aldrich), 1% HEPES buffer (Gibco) and 1% GlutaMAX (Gibco), 20% R-spondin1 conditioned medium, 10% Noggin conditioned medium, 2% B27 (Fisher Scientific), 1.25 mM N-acetyl cysteine (Sigma-Aldrich) and 50µg/ml EGF (Peprotech). Wnt culture medium (WENR) contained ENR medium, with 50% R-spondin1 conditioned medium in total, and supplemented Wnt Surrogate-Fc fusion protein (U-protein Express, N001) at 1:15.000 or 1:20.000. Organoids were cultured at 37°C under a 5% CO_2 atmosphere.

Plasmids and lentiviral transduction

HyPer7 without localisation and HyPer7-NLS, -NES, -MLS, -IMS, -LifeAct, -FS sequences were a gift from dr. Belousov (Pak et al., 2020). HyPer7-LifeAct is localised to actin, and HyPer7-FS is localised to the cytosolic side of the membrane by a farnesylation tag of GTPase HRAS. The sequences were isolated using PCR (Polymerase Chain Reaction) and were cloned into a lentiviral backbone by infusion cloning with primers designed in SnapGene (see Table 1). The pLV-H2B-mNeon-ires-Puro backbone was used, where the puromycin resistance cassette was replaced by a blasticidine resistance gene. PCR products were loaded on a 1% agarose gel, after which remaining PCR products were purified using a miniprep kit (Qiagen). The backbone was linearised by restriction digestion with BstBI and NheI (New England Biolabs), after which the PCR products were ligated into the backbone using the In-Fusion HD cloning kit (Takara), according to manufacturer's protocol. Then, the plasmids were grown in *E.coli* DH5α with ampicillin, after which the samples were purified using a miniprep kit (Qiagen). Samples were sent for sequencing, using the forward primers of infusion cloning, a reverse primer located in the HyPer7 gene,

and a reverse primer in the IRES to verify whether HyPer7 was cloned correctly into the backbone. After verifying the correctly cloned constructs, the respective bacteria were grown out and plasmids were purified using a maxiprep kit (Qiagen). The lentiviral constructs were transfected into HEK293T cells with PEI (Sigma Aldrich), together with third-generation packaging vectors. After two days of culturing, the medium of HEK293T containing virus was filtered (0.45μm) and virus was concentrated using ultracentrifugation.

Primer	Sequence
HyPer7 FW	5' GTACCGATAGCTTCGAAGCCACCATGCACCTGGCTAATGAGG 3'
HyPer7-IMS FW	5' GTACCGATAGCTTCGAAGCCACCATGGCGGCTCTGAAGAG 3'
HyPer7-LifeAct FW	5' GTACCGATAGCTTCGAAGCCACCATGGGCGTGG 3'
HyPer7-MLS FW	5' GTACCGATAGCTTCGAAGCAGGATCCCATCGATTCGAA 3'
HyPer7 RV	5' ATGGCACTAGGCTAGCTCAATCGCAGATGAAGCTAACACCATGC 3'
HyPer7-NES RV	5' ATGGCACTAGGCTAGCTTACAGGGTCAGCCGCTCCAGG 3'
HyPer7-NLS RV	5' ATGGCACTAGGCTAGCCTAGAGGCTCGAGTTATACCTTTCTCT 3'
HyPer7-LifeAct RV	5' ATGGCACTAGGCTAGCTCAATCGCAGATGAAGCTAACACC 3'
HyPer7-FS RV	5' ATGGCACTAGGCTAGCTTAGGAGAGCACACACTTGCAGC 3'
IRES RV	5' CTTCGGCCAGTAACGTTAGG 3'
Begin-HyPer7 RV	5' ATACCCGGCTCTTGAAACG 3'

Table 1 – Primers used for Infusion cloning

MDCK and RPE^Tert cells were infected with the lentiviral HyPer7 constructs in presence of polybrene (1:1000; Sigma Aldrich), and selected with Blasticidin (3μg/ml – MDCK, 20μg/ml - RPE; Invivogen). After, cells were single sorted using Fluorescence Activated Cell Sorting and grown out monoclonally in conditioned medium (1:1), however, RPE-HyPer7 IMS and -MLS did not grow out monoclonally.

Before lentiviral transduction, organoids were placed on WENR medium for 3-4 days, in order for the organoids to grow cystic and contain more proliferating cells. On the day of infection, organoids were treated with TripLE (Gibco) to form small clumps of cells. Then organoids were infected by spinoculation at room temperature at 600 rpm for 1h with the lentiviral HyPer7-NES and -NLS constructs, in presence of culture medium, polybrene (1:1000) and Y-27632 (1:1000; Gentaur). After spinoculation, organoids with the infection medium were placed in the incubator for at least 4 hours, before being plated in BME and grown in WENR medium, with 0,1% Y-27632. After 1 day, organoids were selected and maintained with 50 μg/ml blasticidin. After several days, Wnt was removed from the medium to promote cryptic outgrowth again.

HAP1 cells were infected with H2B-mScarlet-DAAO and TOM20-mScarlet DAAO lentiviral constructs in presence of polybrene (1:1000) and selected with puromycin (750ng/ml, Bio-connect). After, cells were single sorted using cellenONE and grown out monoclonally in conditioned medium (1:1).

Correct localisation of the constructs was confirmed by fluorescence microscopy. For HyPer7-IMS and -MLS MDCK cells, mitochondrial localisation was validated with a mitochondrial dye. MDCK HyPer7-IMS and -MLS cells were plated in a glass bottom dish, coated with 0.05% Rat Tail Type I Collagen (Corning) in 0.1% acetic acid. Tetramethylrhodamine, Methyl Ester, Perchlorate (TMRM; Invitrogen), was administered to the cells 30 minutes prior to imaging, according to manufacturer's protocol. Cells were imaged on a Zeiss LSM 880 laser scanning confocal microscope with 100x magnification, in a 37°C, 6% CO_2 environment. HyPer7 was imaged with 488nm excitation and detected at 498-570nm, TMRM was imaged at 561nm excitation and detected at 590-700nm.

Immunofluorescence microscopy

MDCK WT cysts were grown for 5 days, and fixed in 4% paraformaldehyde (PFA; electron microscopy sciences) in PBS for 15 minutes at 4°C. Fixed cysts were washed twice with phosphate buffered saline (PBS), and permeabilised for 4 hours in PBD2T buffer (1% BSA (w/v), 10% DMSO, 2% Triton x-100 in PBS). Then, the cysts were incubated with PBD2T with primary antibodies (DECMA-1 (1:1000; Rat Genetex GTX1151)), overnight, followed by 5x washing with PBS, and PBD2T with secondary antibodies (Phalloidin 488 (1:500; A22287, ThermoFisher), anti-rat Alexa fluor 647 (1:500; A21247, ThermoFisher), DAPI (1:1000), Sigma Aldrich)) overnight. All antibody incubations were performed at 4 °C and in the dark. Before imaging, cells were washed 5x with PBS and left with PBS for imaging. Imaging was performed on a Zeiss LSM 880 laser scanning confocal microscope with 40x magnification. DAPI was excited at 405nm and detected at 410-603nm, Phalloidin 488 was excited at 488nm and detected at 493-675nm, and Alexa 647 was excited at 633 nm and detected at 638-753nm.

Live imaging of MDCK cysts and organoids

MDCK HyPer7-NES, -NLS, -MLS, -IMS cysts in LabTek were imaged using a Zeiss LSM 880 laser scanning confocal microscope with 20x magnification, in a 37°C, 6% CO_2 environment. HyPer7 was imaged with 405 and 488nm excitation consecutively and detected at 493-570nm. Images were taken at an interval of 5 minutes for H_2O_2 titrations, or an interval of 15, 20 or 30 minutes for menadione and paraquat treatments. Different treatments were added after measuring the first timepoint. Compounds used are: Paraquat (Sigma Aldrich), Menadione (Sigma Aldrich) or H_2O_2 (Sigma Aldrich).

MSI HyPer7-NES and -NLS organoids were plated in a droplet of Matrigel in a LabTek 8-wells chamber slide with culture medium was added. The organoids were imaged in the same way as the cysts. No treatment was added.

Images were processed and analysed using FIJI imaging software. Background signal of cells without HyPer7 was subtracted from HyPer7-NLS images; for the other experiments, this was not performed. Images were thresholded to remove background pixels, upon which the ratio of $488nm_{ex}/405nm_{ex}$ was determined. For analysis, the mean grey value of separate cysts was calculated and normalised to the first timepoint. The values were depicted into graphs using GraphPad Prism 8 Software and the standard deviation was determined.

Flow Cytometry after 5-FU treatment

RPE HyPer7-NES and NLS cells were plated in a 6-wells dish the day before treatment. Cells were treated with different concentrations of 5-FU (Sigma Aldrich) dissolved in DMSO or just DMSO for 4h or approx. 18h. 15 or 30 minutes before fixation, cells were treated with H_2O_2. Before fixation, cells were washed with warm PBS containing 50mM NEM (Sigma Aldrich), to prevent oxidation or reduction of HyPer7 due to harvesting. Cells were then fixed with 4% PFA in PBS for 10 minutes at room temperature. After, the PFA was washed away with PBS twice, after which the samples were resuspended in PBS buffer with 1% BSA and 0.05% Tween. Then, the samples were analysed on a FACSCelesta Flow Cytometer (BD Bioscience). HyPer7 was measured using Ex405/Em525/50 and Ex488/Em30/30 lasers and filter sets. Flow cytometry data was analysed using BD FACSDiva Software, and geometric means were used to determine the HyPer7 ratio. Values were depicted into graphs using GraphPad Prism 8 Software.

Live imaging with 5-FU treatment

RPE HyPer7-NES and -NLS cells were plated in 8-well chamber slides (ibidi) and imaged using a Zeiss Cell Observer microscope with 10x magnification, in a 37°C, 6% CO_2 environment. HyPer7 was excited with 385nm and 499nm, and emission was detected from 492-536nm. Images were taken at an interval of

20 minutes. 5-FU and H_2O_2 treatments were added after measuring the first timepoint. Images were processed and analysed using FIJI imaging software. Images were thresholded to remove the background pixels, upon which the ratio of $499nm_{ex}/485nm_{ex}$ was determined. For analysis, the mean grey value of the cells in view (approx. 250 cells) and normalised to the first timepoint. The values were depicted into graphs using GraphPad Prism 8 Software.

<u>HAP1-DAAO characterisation</u>

HAP1 DAAO-TOM20 and -H2B cells were plated in a 6-wells dish the day before treatment. Cells were treated for 48 hours with different concentrations of D-alanine (Sigma Aldrich) and L-alanine (Sigma Aldrich) as a control, after which they were assessed with different procedures.

For the crystal violet staining, cells were washed with cold PBS, after which the cells were fixed with -20°C 100% methanol for more than 5 minutes. Methanol was aspirated, and crystal violet solution (0.5% w/v in 25% v/v methanol) was added at room temperature for 10 minutes. After staining, plates were washed with demi water and left to air dry overnight. Plates were photo scanned to create an image.

Cell death was determined using propidium iodide (PI) exclusion. Media on the cells was harvested to take along floating cells. Cells were washed with PBS and was also taken along, together with cells after trypsinisation. The mixture of cells was washed with PBS, and then resuspended in PBS with 0,02 mg/ml PI (Sigma Aldrich). Cells were analysed on a FACSCelesta Flow Cytometer (BD Bioscience). PI was measured with the 568 laser and PE filter sets. Flow cytometry data was analysed using BD FACSDiva Software and the population of PI positive (dead) cells and negative (alive) cells was determined. The ratio alive/(dead+alive) was calculated and values were depicted into graphs using GraphPad Prism 8 Software.

For cell cycle profile assessment, plates were washed with PBS, and cells were harvested after trypsinisation. Cells were fixed with -20°C 70% ethanol while vortexing, and stored at 4°C overnight. Ethanol was removed and cells were resuspended in staining buffer (PBS with 0,02 mg/ml PI and 5 µl RNAse (Fuji Film Wako Chemicals), after which cells were analysed on a FACSCelesta Flow Cytometer (BD Bioscience). PI was measured with the PE laser and filter sets. Flow cytometry data was analysed using BD FACSDiva Software and histograms for PE were made.

Acknowledgements

References

Abo, M., & Weerapana, E. (2019). Chemical Probes for Redox Signaling and Oxidative Stress. *Antioxidants & Redox Signaling*, *30*(10), 1369. https://doi.org/10.1089/ARS.2017.7408

Ames, B. N., Shigenaga, M. K., & Hagen, T. M. (1993). Oxidants, antioxidants, and the degenerative diseases of aging. *Proceedings of the National Academy of Sciences*, *90*(17), 7915–7922. https://doi.org/10.1073/PNAS.90.17.7915

Beigl, T. B., Kjosås, I., Seljeseth, E., Glomnes, N., & Aksnes, H. (2020). Efficient and crucial quality control of HAP1 cell ploidy status. *Biology Open*, *9*(11). https://doi.org/10.1242/BIO.057174

Bilan, D., & Belousov, V. (2016). HyPer Family Probes: State of the Art. *Antioxidants & Redox Signaling*, *24*(13), 731–751. https://doi.org/10.1089/ARS.2015.6586

Bogdanova, Y. A., Schultz, C., & Belousov, V. V. (2017). Local Generation and Imaging of Hydrogen Peroxide in Living Cells. *Current Protocols in Chemical Biology*, *9*(2), 117–127. https://doi.org/10.1002/CPCH.20

Carette, J. E., Guimaraes, C. P., Varadarajan, M., Park, A. S., Wuethrich, I., Godarova, A., Kotecki, M., Cochran, B. H., Spooner, E., Ploegh, H. L., & Brummelkamp, T. R. (2009). Haploid Genetic Screens in Human Cells Identify Host Factors Used by Pathogens. *Science*, *326*(5957), 1231–1235. https://doi.org/10.1126/SCIENCE.1178955

Carette, J. E., Raaben, M., Wong, A. C., Herbert, A. S., Obernosterer, G., Mulherkar, N., Kuehne, A. I., Kranzusch, P. J., Griffin, A. M., Ruthel, G., Cin, P. D., Dye, J. M., Whelan, S. P., Chandran, K., & Brummelkamp, T. R. (2011). Ebola virus entry requires the cholesterol transporter Niemann–Pick C1. *Nature 2011 477:7364*, *477*(7364), 340–343. https://doi.org/10.1038/NATURE10348

Christensen, S., Van der Roest, B., Besselink, N., Janssen, R., Boymans, S., Martens, J. W. M., Yaspo, M.-L., Priestley, P., Kuijk, E., Cuppen, E., & Van Hoeck, A. (2019). 5-Fluorouracil treatment induces characteristic T>G mutations in human cancer. *Nature Communications 2019 10:1*, *10*(1), 1–11. https://doi.org/10.1038/S41467-019-12594-8

Cochemé, H., & Murphy, M. (2008). Complex I is the major site of mitochondrial superoxide production by paraquat. *The Journal of Biological Chemistry*, *283*(4), 1786–1798. https://doi.org/10.1074/JBC.M708597200

D'Autréaux, B., & Toledano, M. B. (2007). ROS as signalling molecules: Mechanisms that generate specificity in ROS homeostasis. In *Nature Reviews Molecular Cell Biology* (Vol. 8, Issue 10, pp. 813–824). Nature Publishing Group. https://doi.org/10.1038/nrm2256

De Henau, S., Pagès-Gallego, M., Pannekoek, W. J., & Dansen, T. B. (2020). Mitochondria-Derived H2O2 Promotes Symmetry Breaking of the C. elegans Zygote. *Developmental Cell*, *53*(3), 263-271.e6. https://doi.org/10.1016/J.DEVCEL.2020.03.008

Focaccetti, C., Bruno, A., Magnani, E., Bartolini, D., Principi, E., Dallaglio, K., Bucci, E., Finzi, G., Sessa, F., Noonan, D., & Albini, A. (2015). Effects of 5-fluorouracil on morphology, cell cycle, proliferation, apoptosis, autophagy and ROS production in endothelial cells and cardiomyocytes. *PloS One*, *10*(2). https://doi.org/10.1371/JOURNAL.PONE.0115686

Forman, H. J., Ursini, F., & Maiorino, M. (2014). An overview of mechanisms of redox signaling. In *Journal of Molecular and Cellular Cardiology* (Vol. 73, pp. 2–9). Academic Press. https://doi.org/10.1016/j.yjmcc.2014.01.018

Güçlü, H., Doganlar, Z., Gürlü, V., Özal, A., Dogan, A., Turhan, M., & Doganlar, O. (2018). Effects of cisplatin-5-fluorouracil combination therapy on oxidative stress, DNA damage, mitochondrial

apoptosis, and death receptor signalling in retinal pigment epithelium cells. *Cutaneous and Ocular Toxicology*, *37*(3), 291–304. https://doi.org/10.1080/15569527.2018.1456548

Halvey, P., Hansen, J., Johnson, J., Go, Y., Samali, A., & Jones, D. (2007). Selective oxidative stress in cell nuclei by nuclear-targeted D-amino acid oxidase. *Antioxidants & Redox Signaling*, *9*(7), 807–816. https://doi.org/10.1089/ARS.2007.1526

Hansen, J. M., Jones, D. P., & Harris, C. (2020). The Redox Theory of Development. *Antioxidants & Redox Signaling*, *32*(10), 715–740. https://doi.org/10.1089/ARS.2019.7976

Hebbar, S., & Knust, E. (2021). Reactive oxygen species (ROS) constitute an additional player in regulating epithelial development. *BioEssays*, *43*(8), 2100096. https://doi.org/10.1002/BIES.202100096

Holmström, K. M., & Finkel, T. (2014). Cellular mechanisms and physiological consequences of redox-dependent signalling. *Nature Reviews Molecular Cell Biology 2014 15:6*, *15*(6), 411–421. https://doi.org/10.1038/NRM3801

Hu, J., Dong, L., & Outten, C. E. (2008). The Redox Environment in the Mitochondrial Intermembrane Space Is Maintained Separately from the Cytosol and Matrix. *Journal of Biological Chemistry*, *283*(43), 29126–29134. https://doi.org/10.1074/JBC.M803028200

Hunter, M. V., Willoughby, P. M., Bruce, A. E. E., & Fernandez-Gonzalez, R. (2018). Oxidative Stress Orchestrates Cell Polarity to Promote Embryonic Wound Healing. *Developmental Cell*, *47*(3), 377-387.e4. https://doi.org/10.1016/J.DEVCEL.2018.10.013

Koçer, M., & Nazıroğlu, M. (2013). Effects of 5-Fluorouracil on Oxidative Stress and Calcium Levels in the Blood of Patients with Newly Diagnosed Colorectal Cancer. *Biological Trace Element Research 2013 155:3*, *155*(3), 327–332. https://doi.org/10.1007/S12011-013-9795-4

Kritsiligkou, P., Shen, T. K., & Dick, T. P. (2021). A comparison of Prx- and OxyR-based H2O2 probes expressed in S. cerevisiae. *The Journal of Biological Chemistry*, *297*(1). https://doi.org/10.1016/J.JBC.2021.100866

Li, J., Zuo, X., Cheng, P., Ren, X., Sun, S., Xu, J., Holmgren, A., & Lu, J. (2019). The production of reactive oxygen species enhanced with the reduction of menadione by active thioredoxin reductase. *Metallomics*, *11*(9), 1490–1497. https://doi.org/10.1039/C9MT00133F

Longley, D. B., Harkin, D. P., & Johnston, P. G. (2003). 5-Fluorouracil: mechanisms of action and clinical strategies. *Nature Reviews Cancer 2003 3:5*, *3*(5), 330–338. https://doi.org/10.1038/NRC1074

Mailloux, R. J. (2021). An update on methods and approaches for interrogating mitochondrial reactive oxygen species production. *Redox Biology*, *45*, 102044. https://doi.org/10.1016/J.REDOX.2021.102044

Matlashov, M. E., Belousov, V. V., & Enikolopov, G. (2014). How Much H2O2 Is Produced by Recombinant D-Amino Acid Oxidase in Mammalian Cells? *Antioxidants & Redox Signaling*, *20*(7), 1039. https://doi.org/10.1089/ARS.2013.5618

Mavrikou, S., Tsekouras, V., Karageorgou, M., Moschopoulou, G., & Kintzios, S. (2019). Detection of Superoxide Alterations Induced by 5-Fluorouracil on HeLa Cells with a Cell-Based Biosensor. *Biosensors*, *9*(4). https://doi.org/10.3390/BIOS9040126

Nolfi-Donegan, D., Braganza, A., & Shiva, S. (2020). Mitochondrial electron transport chain: Oxidative phosphorylation, oxidant production, and methods of measurement. *Redox Biology*, *37*, 101674. https://doi.org/10.1016/J.REDOX.2020.101674

O'Brien, L., Zegers, M., & Mostov, K. (2002). Opinion: Building epithelial architecture: insights from

three-dimensional culture models. *Nature Reviews. Molecular Cell Biology*, *3*(7), 531–537. https://doi.org/10.1038/NRM859

Olbrich, T., Mayor-Ruiz, C., Vega-Sendino, M., Gomez, C., Ortega, S., Ruiz, S., & Fernandez-Capetillo, O. (2017). A p53-dependent response limits the viability of mammalian haploid cells. *Proceedings of the National Academy of Sciences*, *114*(35), 9367–9372. https://doi.org/10.1073/PNAS.1705133114

Pak, V. V., Ezeriņa, D., Lyublinskaya, O. G., Pedre, B., Tyurin-Kuzmin, P. A., Mishina, N. M., Thauvin, M., Young, D., Wahni, K., Martínez Gache, S. A., Demidovich, A. D., Ermakova, Y. G., Maslova, Y. D., Shokhina, A. G., Eroglu, E., Bilan, D. S., Bogeski, I., Michel, T., Vriz, S., … Belousov, V. V. (2020). Ultrasensitive Genetically Encoded Indicator for Hydrogen Peroxide Identifies Roles for the Oxidant in Cell Migration and Mitochondrial Function. *Cell Metabolism*, *31*(3), 642-653.e6. https://doi.org/10.1016/J.CMET.2020.02.003

Pang, Y., Zhang, H., & Ai, H. (2021). Genetically Encoded Fluorescent Redox Indicators for Unveiling Redox Signaling and Oxidative Toxicity. *Chemical Research in Toxicology*, *34*(8), 1826–1845. https://doi.org/10.1021/ACS.CHEMRESTOX.1C00149

Pollegioni, L., Sacchi, S., & Murtas, G. (2018). Human D-Amino Acid Oxidase: Structure, Function, and Regulation. *Frontiers in Molecular Biosciences*, *0*(NOV), 107. https://doi.org/10.3389/FMOLB.2018.00107

Sato, T., & Clevers, H. (2013). Growing Self-Organizing Mini-Guts from a Single Intestinal Stem Cell: Mechanism and Applications. *Science*, *340*(6137), 1190–1194. https://doi.org/10.1126/SCIENCE.1234852

Schwarzländer, M., Dick, T., Meyer, A., & Morgan, B. (2016). Dissecting Redox Biology Using Fluorescent Protein Sensors. *Antioxidants & Redox Signaling*, *24*(13), 680–712. https://doi.org/10.1089/ARS.2015.6266

Secilmis, M., Altun, H. Y., Pilic, J., Erdogan, Y. C., Cokluk, Z., Ata, B. N., Sevimli, G., Zaki, A. G., Yigit, E. N., Öztürk, G., Malli, R., & Eroglu, E. (2021). A Co-Culture-Based Multiparametric Imaging Technique to Dissect Local H2O2 Signals with Targeted HyPer7. *Biosensors*, *11*(9), 338. https://doi.org/10.3390/BIOS11090338

Sies, H., & Jones, D. P. (2020). Reactive oxygen species (ROS) as pleiotropic physiological signalling agents. In *Nature Reviews Molecular Cell Biology* (Vol. 21, Issue 7, pp. 363–383). Nature Research. https://doi.org/10.1038/s41580-020-0230-3

Stein, K. T., Moon, S. J., & Sikes, H. D. (2018). Mitochondrial H2O2 Generation Using a Tunable Chemogenetic Tool To Perturb Redox Homeostasis in Human Cells and Induce Cell Death. *ACS Synthetic Biology*, *7*(9), 2037–2044. https://doi.org/10.1021/ACSSYNBIO.8B00174

Wang, W., Fang, H., Groom, L., Cheng, A., Zhang, W., Liu, J., Wang, X., Li, K., Han, P., Zheng, M., Yin, J., Wang, W., Mattson, M. P., Kao, J. P. Y., Lakatta, E. G., Sheu, S. S., Ouyang, K., Chen, J., Dirksen, R. T., & Cheng, H. (2008). Superoxide Flashes in Single Mitochondria. *Cell*, *134*(2), 279–290. https://doi.org/10.1016/J.CELL.2008.06.017

Yang, H., Villani, R. M., Wang, H., Simpson, M. J., Roberts, M. S., Tang, M., & Liang, X. (2018). The role of cellular reactive oxygen species in cancer chemotherapy. *Journal of Experimental & Clinical Cancer Research 2018 37:1*, *37*(1), 1–10. https://doi.org/10.1186/S13046-018-0909-X